PULSE COMPRESSION VIA VELOCITY BUNCHING WITH THE LLNL THOMSON X-RAY SOURCE PHOTOINJECTOR

S.G. Anderson*, W.J. Brown, A.M. Tremaine, LLNL, Livermore, CA 94550, USA
P. Musumeci, J.B. Rosenzweig, UCLA, Los Angeles, CA 90095, USA

Abstract

We report the compression of a high brightness, relativistic electron beam to rms lengths below 300 femtoseconds using the velocity compression technique in the LLNL Thomson X-ray source photoinjector. The results are consistent with analytical and computational models of this process. The emittance evolution of the beam during compression is investigated in simulation and found to be controllable with solenoid focusing.

INTRODUCTION

Fourth generation light sources [1] and future high energy physics accelerators [2] will require beams with both very low emittance, and sub-picosecond rms lengths. The need for high brightness motivates the use of radio frequency (rf) photoinjectors, the highest brightness electron sources. However, the brightness of these sources results in space-charge forces which are large enough to dominate the transverse beam dynamics. The method of maintaining the low emittance of photoinjector beams, termed emittance compensation [3, 4], balances the defocusing space-charge forces with external focusing and accelerating forces. This process defines the optimal dimensions of the beam and typically limits the minimum rms bunch length to a few picoseconds.

This limit coupled with the needs of advanced beam applications has produced much interest in the topic of pulse compression of high brightness beams. Specifically, magnetic compression schemes [5], in which a longitudinal position/momentum correlation is created by running off-crest in an rf accelerator and then removed by path-length/momentum correlation in a magnet system, have been studied extensively [6, 7]. These studies have revealed distortions, and corresponding emittance growth, in both the longitudinal and transverse phase space arising from magnetic compression. At moderate to high energy (≥ 40 MeV) coherent synchrotron radiation (CSR) is the most significant source of emittance growth [7], while at lower energies space-charge forces can play an important role [8].

To avoid the effects of magnetic compression on the transverse beam quality, a new rectilinear compression technique, termed velocity bunching, has been proposed [9], and recently studied experimentally [10, 11]. In this paper we review the velocity bunching mechanism and present data produced by its implementation at the LLNL Thomson X-ray source photoinjector [12]. In addition, we examine the beam dynamics in the compression process with PARMELA simulations and find the emittance behavior consistent with that predicted by emittance compensation theory.

* anderson131@llnl.gov

VELOCITY BUNCHING

For compression with velocity bunching, the required time of flight difference between the beam head and tail, $\Delta t/t = \Delta L/L - \Delta v/v$, is provided solely by the velocity difference, $\Delta v/v$, imparted by the time dependent rf fields in the accelerating structure. This method, therefore, is more easily applied at lower energies, since $\Delta v/v = \frac{1}{\gamma^2}(\Delta p/p)$, and the imparted momentum spread required for compression is lower, and may be more easily reduced by acceleration.

To understand the basic mechanism of velocity compression, consider the interaction of an electron with the sinusoidal, accelerating rf wave given by $E_z = E_0 \sin(\Psi)$, where $\Psi = \omega t - kz + \phi_0$ is the particle phase with respect to the wave, and E_0 is the peak accelerating electric field of the wave. With a field of this form, the particle equations of motion are given (as in Ref. [11]) by

$$\frac{d\gamma}{dz} = \alpha k \sin\Psi \qquad (1)$$

$$\frac{d\Psi}{dz} = k\left[\frac{\gamma}{\sqrt{\gamma^2-1}} - 1\right], \qquad (2)$$

where $\alpha = eE_0/m_e c^2 k$ is the dimensionless vector potential amplitude of the wave. These equations can be used to plot electron trajectories in (Ψ, γ) phase space, as illustrated in Fig. 1b. In this space particles follow lines of constant Hamiltonian and, as the figure illustrates, a beam injected near the rf zero crossing ($\Psi = 0$) will initially slip back in phase as a strong Ψ-γ correlation is produced. As the beam slips in phase, it samples a stronger electric field and accelerates as the phase space correlation begins to bunch the beam. At the end of this process the beam has slipped into a strongly accelerating phase and the phase space orientation of the beam has rotated by 90° from that of the injected beam.

EXPERIMENTAL MEASUREMENTS

The LLNL Thomson X-ray source photoinjector and linac consists of a BNL/SLAC/UCLA/LLNL 1.625 cell photo-cathode rf gun [13] followed by four SLAC style 2.5

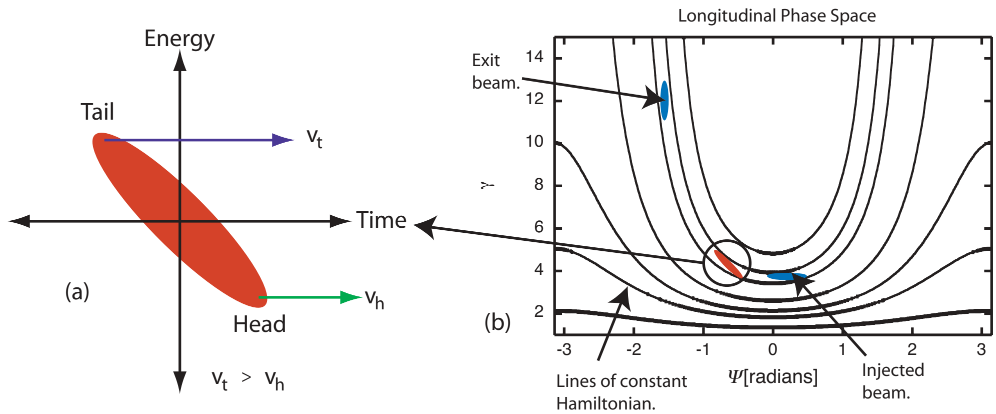

Figure 1: Phase space particle trajectories illustrate the velocity compression mechanism.

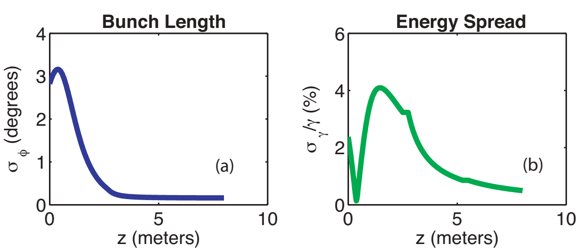

Figure 2: Simulation of the (a) pulse length, and (b) energy spread in the compression experiment.

meter, S-band traveling wave sections. The linac is capable of producing 100 MeV electrons, and is typically run in an energy range of 20-70 MeV for Thomson scattering X-ray production [14]. The gun and each of the accelerator sections are independently powered and phased, allowing us to study velocity compression. The beam charge for this study was 250 pC, again the typical amount produced in X-ray production experiments.

A simulation of longitudinal beam dynamics is shown in Fig. 2. Here the initial phase space configuration is taken from a PARMELA simulation of the rf gun and injected into the first linac section at a phase of $-17°$ ($107°$ ahead of crest). The next two sections are phased in this simulation for on-crest acceleration of the beam up to a final energy of 50 MeV. As the figure shows, the bunch length decreases in the first accelerator section reaching a minimum rms value of 160 femtoseconds. Simultaneously, the energy spread increases to a peak rms value of $\sim$4%. As the beam begins to accelerate at the end of the first section and in the following sections the relative energy spread decreases to a final value of 0.5%. Note also that these simulations predict a final energy of 57 MeV and energy spread of 0.2% when the beam is injected into the first accelerator section at $70°$, consistent with experimental measurements performed with a spectrometer magnet.

The bunch length diagnostic we employed is a polarizing Michelson interferometer which analyzes coherent transition radiation (CTR) emitted from the electron beam's impact on a metal foil [15]. The device uses 100 μm spaced wire grids to polarize the coherent THz radiation, which limits the highest frequencies that can be measured and therefore, limits the shortest measurable pulses to $\simeq$300 femtoseconds, rms.

The first traveling wave section was phased as indicated above to perform the velocity bunching measurement. The phase was adjusted to maximize the CTR detector signal at the end of the linac and thus, minimize the pulse length, since the radiated energy, $E_{CTR} \propto Q^2/\sigma_t$ [16]. The interferometer was then used to obtain the autocorrelation of the electron pulse, shown in Fig 3. Analysis of the interferometer data is complicated somewhat by the fact that longer wavelengths (λ >1 mm) are not adequately measured due to diffraction and finite apertures in the device. The measured data is in fact the filtered autocorrelation of the beam temporal profile. The pulse length was extracted

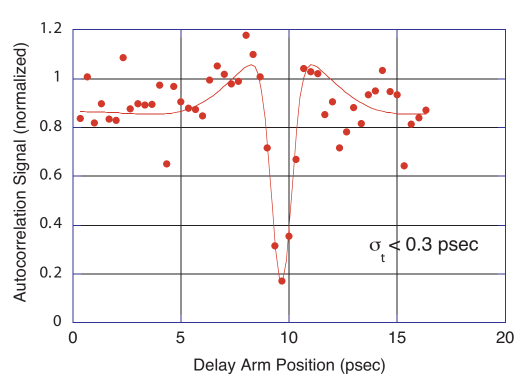

Figure 3: Autocorrelated CTR data for a fully compressed bunch. The measured bunch length is limited by the wavelengths detectable by the diagnostic.

from the data through the use of a time domain fitting algorithm which takes into account the loss of low frequencies, as described in Ref. [15].

The shortest measured pulse length was 300 femtoseconds, rms. This number is consistent with the wire grid spacing limit of the diagnostic and as simulations indicate, the actual bunch length may be significantly shorter. In addition, space-charge inclusive PARMELA and HOMDYN simulations of this system give minimum pulse lengths below 200 fsec.

EMITTANCE DYNAMICS

As mentioned above, velocity bunching has the potential to compress while avoiding the emittance growth observed in bending systems. The possibility for emittance growth in this case comes from space-charge forces. Because the bunch is compressing — increasing in current, in this measurement approaching 1 kA — at relatively low energy, the normal emittance compensation process must be altered to control the emittance.

The nominal emittance compensation process in the case of a split injector [17] is to focus the beam out of the gun to a waist, and matched onto the invariant envelope [4],

$$\sigma_{IE} = \frac{2}{\gamma'}\sqrt{\frac{I}{(1+\eta/2)\,I_0\gamma}}, \qquad (3)$$

at the entrance of the accelerator section. Here γ' is the normalized accelerating gradient, γ the energy, $I_0 = 17$kA the characteristic current, and η is a unitless function of the external focusing forces. In the case of velocity compression, the current increases with z, and we may choose to match the beam to and equilibrium size, σ_{eq} $(\sigma'' = \sigma' = 0)$,

$$\sigma_{eq} = \frac{2}{\gamma'(z)}\sqrt{\frac{2I(z)}{\eta(z)\,\gamma(z)\,I_0}} \qquad (4)$$

If we make the approximation that $I(z)/\gamma(z)$ is constant, then it is clear that the applied external focusing must increase as γ' increases. This process is shown in Fig. 4, where the beam envelope is kept roughly matched by increasing the external solenoid field while it compresses. Here the emittance oscillates, as expected by compensation theory, but does not increase beyond this oscillation.

ACKNOLEDGEMENTS

This work was performed under the auspices of the U.S. Department of Energy by the University of California, Lawrence Livermore National Laboratory under contract No. W-7405-Eng-48.

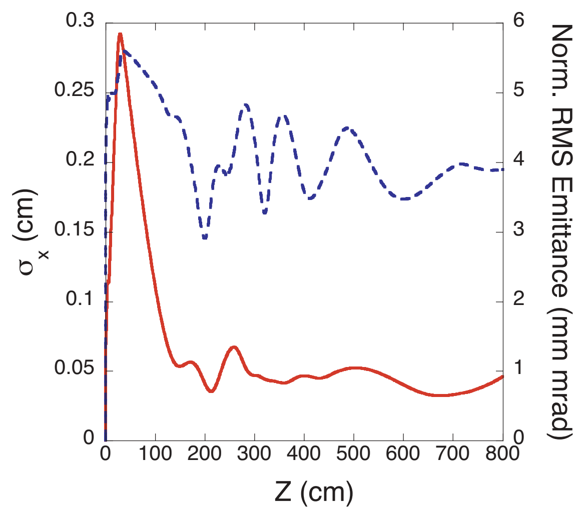

Figure 4: PARMELA simulation of the RMS beam size (solid line) and emittance (dashed line) evolution for the compressing scenario.

REFERENCES

[1] The LCLS Design Study Group, Tech. Rep. SLAC-R-0521, Stanford Linear Accelerator Center (1998).

[2] International Study Group, Tech. Rep. SLAC-R-559, Stanford Linear Accelerator Center (2000).

[3] B. E. Carlsten, Nucl. Instrum. Methods Phys. Res., Sect. A **285**, 313 (1989).

[4] L. Serafini and J. B. Rosenzweig, Phys. Rev. E **55**, 7565 (1997).

[5] M. James *et al.*, IEEE Trans. Nucl. Sci. **NS-30**, 2992 (1983).

[6] H. Braun, *et al.*, Phys. Rev. Lett. **84**, 658 (2000). H. Braun, *et al.*, Phys. Rev. ST Accel. Beams **3**, 124402 (2002).

[7] ICFA Beam Dynamics mini workshop (2002), see `http://www.desy.de/csr/csr_workshop_2002/csr_workshop_2002_index.html`.

[8] S. G. Anderson, Ph. D. thesis, University of California, Los Angeles (2002).

[9] L. Serafini, A. Bacci, and M. Ferrario, in *Proceedings of the PAC 2001, Chicago*, (IEEE, Piscataway, NJ, 2001), pp. 2242-2244.

[10] P. Musumeci *et al.*, these proceedings.

[11] P. Piot *et al.*, Phys. Rev. ST Accel. Beams **6**, 033503 (2003).

[12] G. P. LeSage *et al.*, in *Advanced Accelerator Concepts: Ninth Workshop*, edited by P.L. Colestock and S. Kelly (AIP, New York, 2001), AIP Conf. Proc. No. 569.

[13] D. T. Palmer, Ph. D. thesis, Stanford University (1998).

[14] W. J. Brown *et al.*, these proceedings.

[15] A. Murokh *et al.*, Nucl. Instrum. Methods Phys. Res., Sect. A **410**, 452 (1998).

[16] A. Murokh, Ph. D. thesis, University of California, Los Angeles (2002).

[17] L. Serafini and J.B. Rosenzweig, in *Proceedings of the PAC 1997*, (IEEE, Piscataway, NJ, 1997), p. 2876.